# A PHYSICAL COMPARISON OF VERSION 5 TRMM PR AND TMI RAINFALL ESTIMATES WITH EACH OTHER AND RAIN GAUGE NETWORKS ON GLOBAL, REGIONAL, AND STORM SCALES

Stephen W. Nesbitt*[†], Chuntao Liu[◊], Galdino V. Mota[°],
David Gochis[‡], Edward J. Zipser[◊], and Christian Kummerow[†]

[†]Colorado State University, Fort Collins, Colorado, USA
[◊]University of Utah, Salt Lake City, Utah, USA
[°]Federal University of Para, Belem, Para, Brazil
[‡]National Center for Atmospheric Research, Boulder, CO, USA

## 1. INTRODUCTION

This study relates findings regarding comparisons of version 5 TRMM rainfall estimates with each other and rain gauge networks globally (from the GPCC, Nesbitt et al. 2004) and high-resolution networks over Brazil (Mota 2003) and Mexico (Nesbitt et al. 2004, Gochis et al. 2004).

## 2. BRAZIL

Figure 1 shows rainfall over South America according to the PR, TMIConsistent with previous works (e.g. Kummerow et al. 2001), TMI rainfall is found to be higher than PR rainfall in most Tropical areas, with a bias sign reversal at mid-latitudes between the PR and TMI over the area dominated by MCSs over the La Plata basin.

Over the Andes, both the PR and TMI indicate a local precipitation maximum that is not present in the sparse GPCC gauge network there.

## 3. NORTHWEST MEXICO

Figure 2 shows the JJA 0.5° x 0.5° 6-year climatology of rainfall (mm/day) from the TRMM Microwave Imager (a) and Precipitation Radar (b) over the North American Monsoon Experiment Tier-1 domain, as well as TMI-PR (mm/day) in (c).

Note the large differences with TMI > PR over the western foothills of the SMO (by as much as 10 mm/day). Interestingly, the sign of the differences reverses as one progresses to the high peaks of the SMO, with points to the east of the ridge line having PR estimates > than the TMI (by 4-6 mm/day). These differences easily exceed a 100 percent difference in both directions within many heavily raining areas. Monthly gridded rainfall in coastal, foothill, and mountain locations is plotted in Figure 3 differs greatly by location and month.

## 4. TRMM VS. GPCC GAUGES TROPICS-WIDE

Comparisons of the rain estimates on long temporal scales and large spatial scales can be used in a broad sense to help to mitigate the effects of random error to show algorithmic biases. Figure 3 compares the December 1997–November 2001 2.5º x 2.5º rain estimates on a log–log scale from the TMI, PR, and GPCC gauge analyses in grid boxes with at least one gauge (graydots) and boxes with at least five gauges (black circles).

Means of the two datasets appear in each panel. In Fig. 3a, the TMI estimates are found to be 16% higher than the PR Tropics-wide over land where one gauge exists, which is roughly consistent with the 20% figure quoted by Kummerow et al. (2001) given the different locations and time periods used. In areas with five gauges, the TMI is only 7% higher, but this result is likely due to the locations of sample points in the subtropics (see Fig. 1); the fractional bias is highest in the deep Tropics (Kummerow et al. 2001). The PR estimates more rainfall at lower rain rates, with the exception of a few outliers where the TMI is several factors greater than the PR. At higher rain rates, the TMI generally estimates more rainfall. In comparing the PR with the GPCC gauges in Fig. 3b, it is seen that the GPCC gauges are about 2% and 3% higher than the PR in locations with at least one and five gauges, respectively. The TMI estimates are about 16% and 9% higher than the GPCC estimates (Fig. 3c) for the two gauge number thresholds, respectively.

To show the geographic distribution of the estimates and their differences, Fig. 5 shows the rain estimates and their differences for the same 4-yr period shown in the scatterplots over both the land and ocean, where available. Note in Fig. 3 that the rain estimates differ significantly as portrayed in the scatterplots in Fig. 4. The figure shows that the estimates agree in a qualitative sense, with the gauges (Fig. 5a) and PR (Fig. 5b) underestimating with respect to the TMI (Fig. 5c), especially in the deep Tropics. These disparities show up in the difference maps as well (Figs. 5d–f), where the TMI has more than 2 times the PR estimates over land areas like the Martitime Continent, equatorial Africa, tropical Australia, and the coastline areas in Chile, Baja California, western Africa, and the Middle East. The latter coastline problems are due to a screening problem in the TMI algorithm in which artifacts arise because of the coastline discontinuity in the algorithm (i.e., the transition between land and ocean algorithms). Over the ocean, large TMI positive differences show up over the Pacific ITCZ, and the percentage differences are higher in the central and eastern Pacific than in the western Pacific (not shown) because of lower rain rates in the east (Berg et al. 2002). Lesser positive TMI–PR differences (of >40%) exist over large areas of the Amazon basin, and the Atlantic and Indian Ocean ITCZ.

On the contrary, the PR exceeds the TMI in several higher-latitude land regions, including inland areas in China, Mexico, and the United States, and South America, Africa, and Australia south of 30ºS, as well as dry regions like North Africa, the Middle East, and ocean areas dominated by subtropical highs. The poster will reveal further results and discussion on these issues.


Kummerow, C., and Coauthors, 2001: The evolution of the Goddard profiling algorithm (GPROF) for rainfall estimation from passive microwave sensors. *J. Appl. Meteor.,* **40,** 1801–1820.

Mota, G. V., 2003: Characteristics of rainfall and precipitation features defined by the Tropical Rainfall Measuring Mission over South America. Ph.D. dissertation, University of Utah, 215 pp.Nesbitt, S. W., T. J. Lang, Cifelli, R., Gochis, D., and S. A. Rutledge, 2004: Rainfall in the North American Monsoon Tier-1 domain. Poster, 1st CLIVAR International Science Conference, Baltimore, MD.

Nesbitt, S. W., E. J. Zipser, and C. Kummerow, 2004: An examination of version-5 rainfall estimates from the TRMM microwave imager,
precipitation radar, and rain gauges on global, regional, and storm scales. *J. Climate*, **43**, 1016-1036.


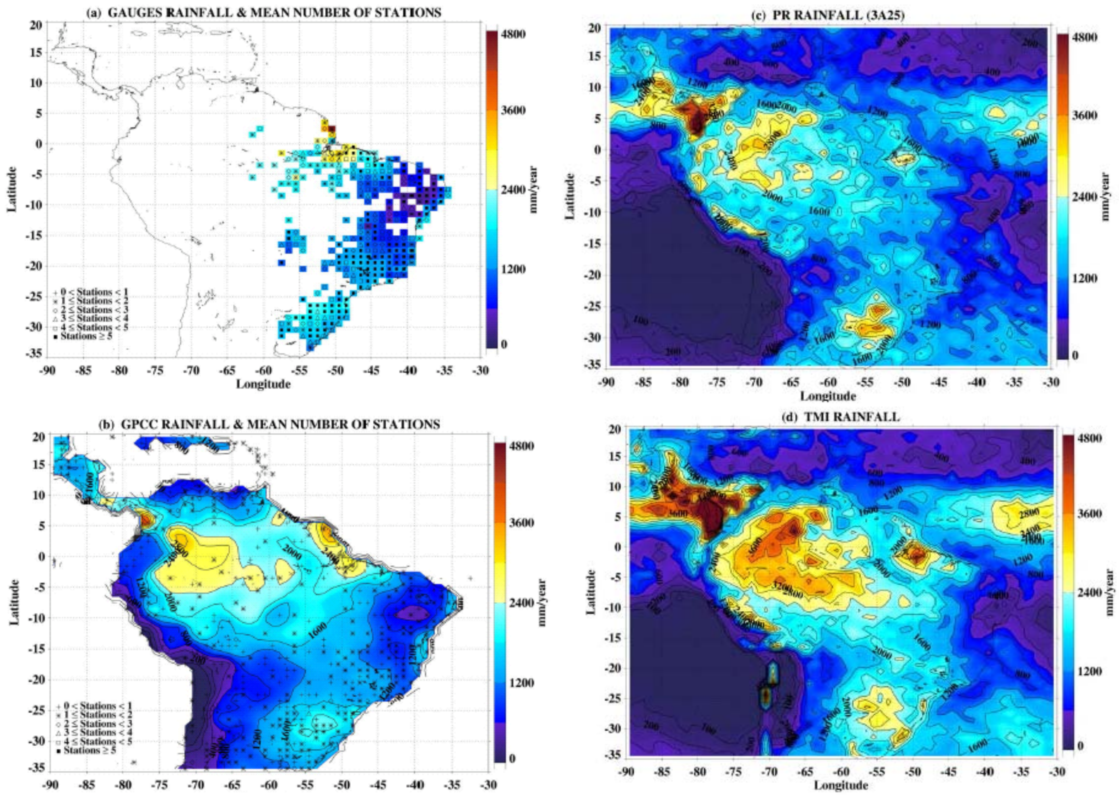


Figure 1. Three years of (a) Brazilian and (b) GPCC rain gauge, (c) PR, and (d) TMI rain accumulations (mm/month).

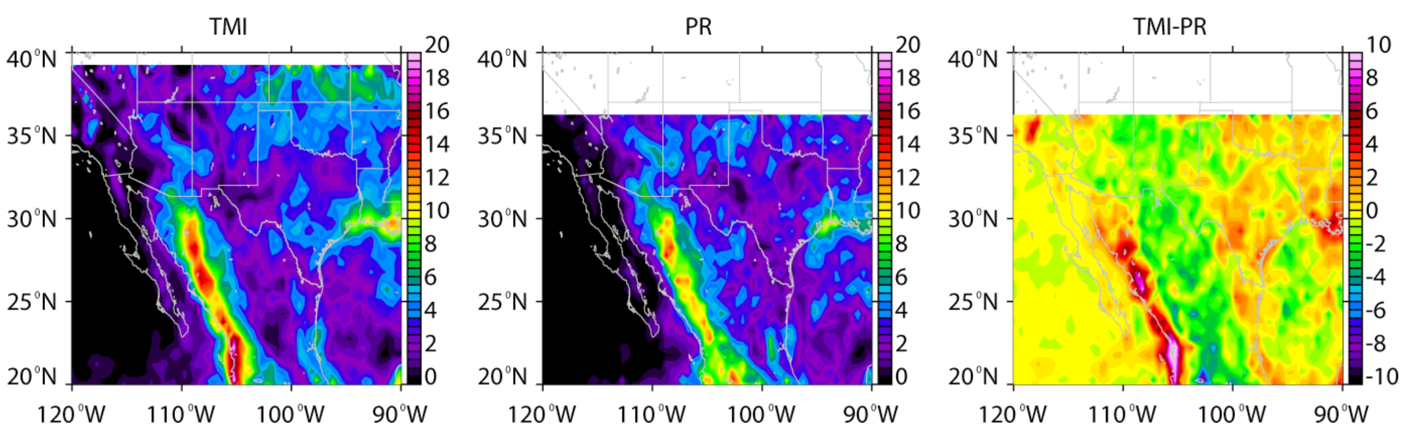


Figure 2. TRMM microwave imager (TMI, left) and precipitation radar (PR, center) 1998-2003 June-August rainfall estimates (mm/day), (c) TMI-PR (mm/day, right).

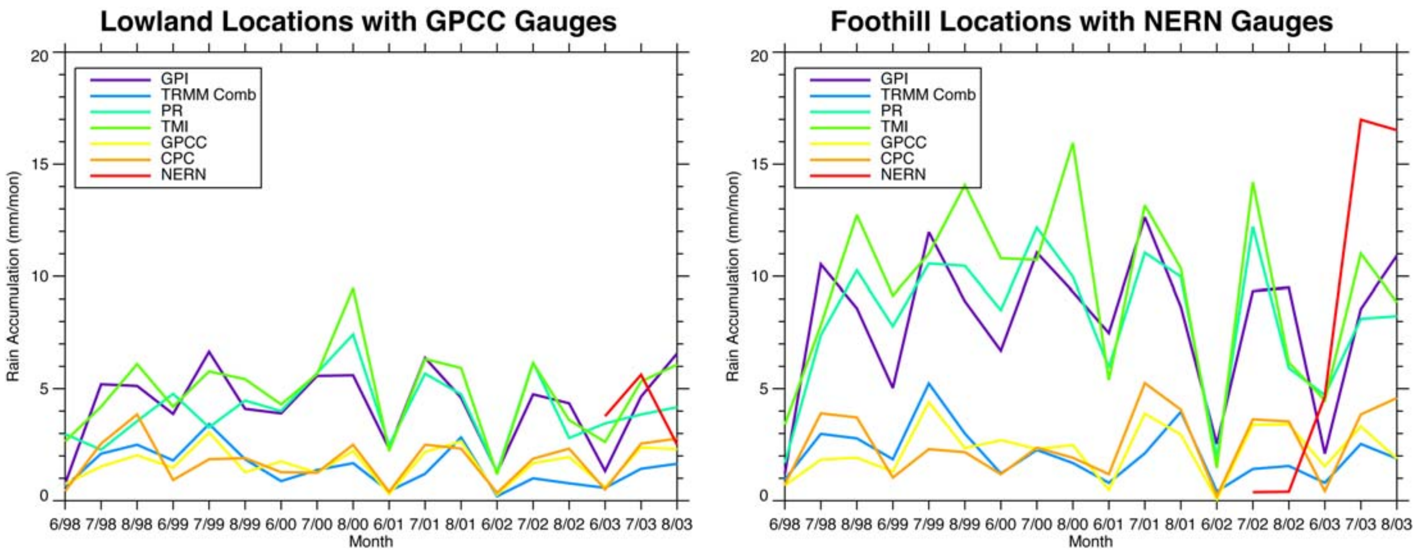


Figure 3. Gridded 1 degree comparisons of warm season rainfall for the rainfall estimates shown in the legend for selected lowand locations (upper left-4 grid boxes), foothill locations (upper right-6 grid boxes), and mountain locations (lower right-7 grid boxes) with NERN rain gauges.

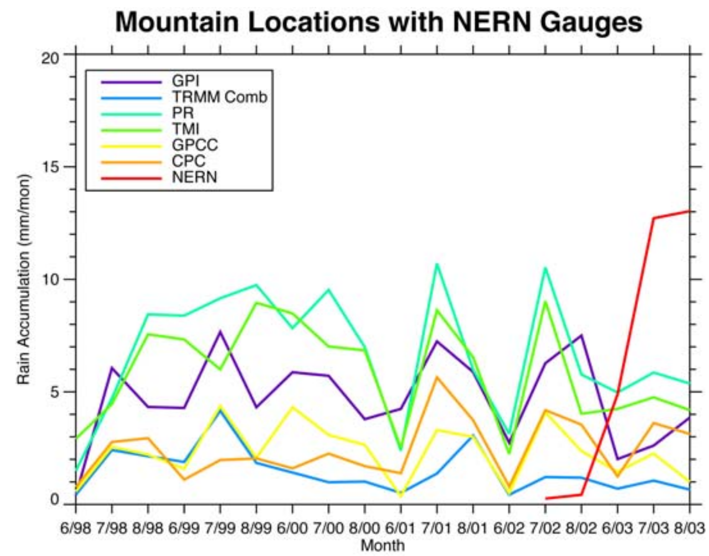


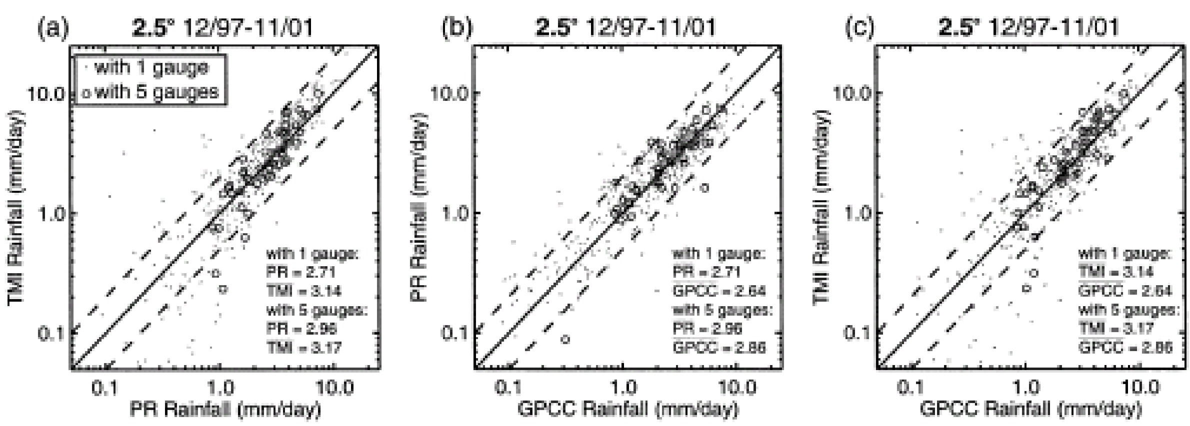


Figure 4. Scatterplots of 2.5 deg x 2.5 deg (a) TMI vs PR, (b) PR vs GPCC, and (c) TMI vs GPCC rainfall in grid boxes with at least one gauge (gray dots) and five gauges (open circles). Note the log–log axis; the solid line is the 1:1 line, and the dashed lines indicate a 100% difference. Mean rainfall values (mm/day) for each gauge number threshold are displayed.

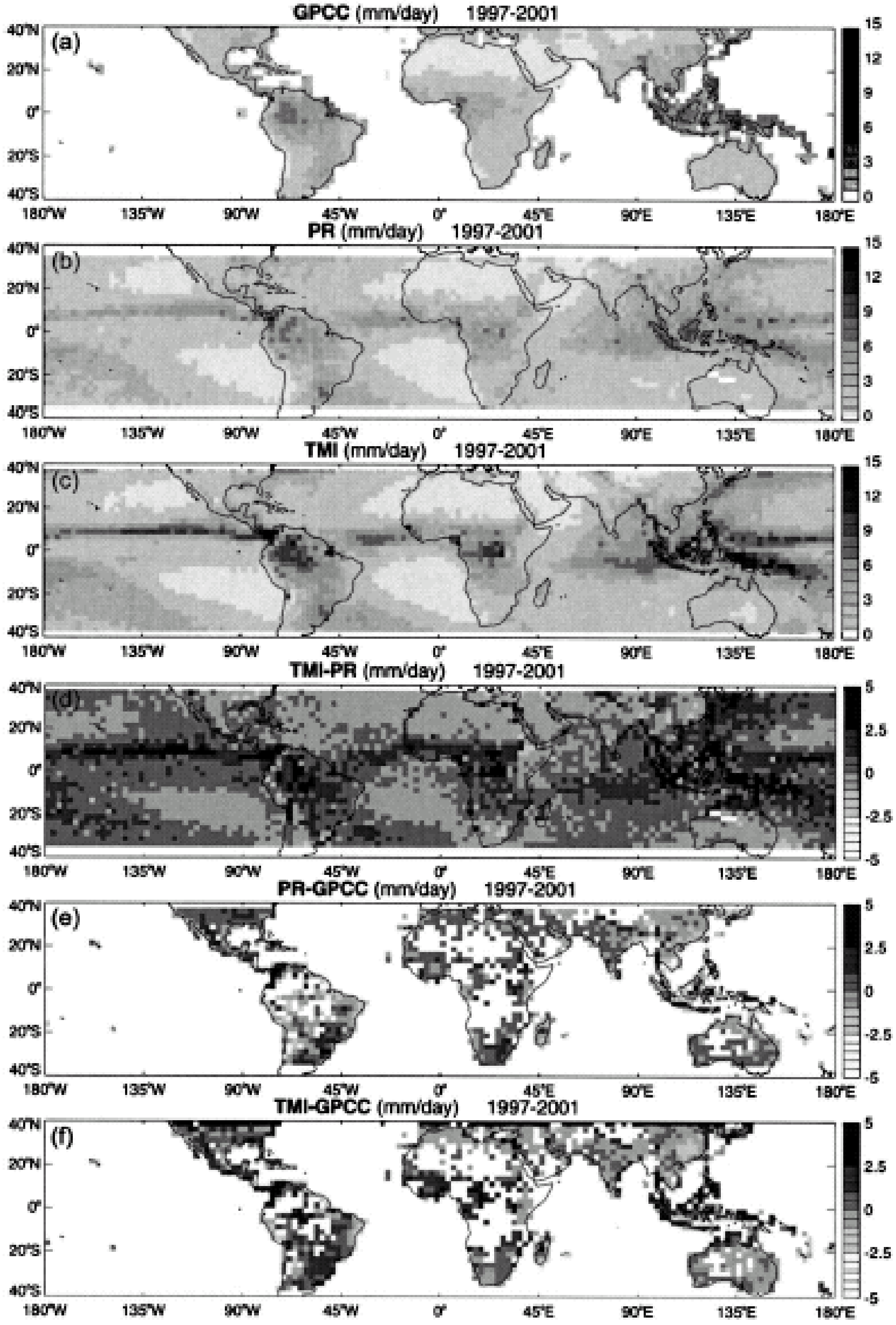


Figure 5. Mean daily 2.5 deg x 2.5 deg rain estimates and differences for all seasons for the period of Dec 1997–Nov 2001. (a) PR, (b) TMI, and (c) GPCC rainfall (mm/day), and differences (mm/day) between the (d) PR and TMI, (e) PR and GPCC, and (f ) TMI and GPCC. White areas indicate (a)–(d) no data and (e)–(f ) less than one gauge.